Available online at www.sciencedirect.com
SCIENCE DIRECT®
Journal of Solid State Chemistry 174 (2003) 296–301
JOURNAL OF SOLID STATE CHEMISTRY
http://elsevier.com/locate/jssc

Synthesis, structure, and magnetism of a new heavy-fermion antiferromagnet, $CePdGa_6$

Robin T. Macaluso,[a] S. Nakatsuji,[b] H. Lee,[b] Z. Fisk,[b] M. Moldovan,[c] D.P. Young,[c] and Julia Y. Chan[a,*]

[a] *Department of Chemistry, Louisiana State University, 232 Choppin Hall, Baton Rouge, LA 70803, USA*
[b] *National High Magnetic Field Laboratory, Florida State University, Tallahassee, FL 32306, USA*
[c] *Department of Physics and Astronomy, Louisiana State University, Baton Rouge, LA 70803, USA*

Received 28 January 2003; received in revised form 7 April 2003; accepted 17 April 2003

Abstract

A new compound, $CePdGa_6$, and its isostructural analog, $LaPdGa_6$ have been synthesized by flux growth and characterized by single-crystal X-ray diffraction. The compounds adopt a tetragonal structure with $P4/mmm$ space group, $Z = 1$. The lattice parameters for $CePdGa_6$ are $a = b = 4.350(3)$ Å and $c = 7.922(6)$ Å and $a = b = 4.3760(3)$ Å and $c = 7.9230(5)$ Å for $LaPdGa_6$. Magnetic and thermal measurement have revealed that $CePdGa_6$ is a heavy-fermion with the specific heat coefficient $\gamma \sim 300$ mJ/mol K^2 and Ce f moments order antiferromagnetically along c-axis at $T_N = 10$ K. Reconfiguration of spin occurs at 5 K to induce a ferromagnetic component only in the a–b plane. This strong anisotropy in the magnetism might be related to its unique layered structure.
© 2003 Elsevier Inc. All rights reserved.

Keywords: $CePdGa_6$; Single-crystal X-ray diffraction; Heavy-fermion; Metamagnetism

1. Introduction

Ternary intermetallic compounds, Ln-T-X, consisting of a (Ln) lanthanide, (T) transition metal, and a (X) main group metal exhibit fascinating physical properties. Some of these are heavy-fermion materials, which exhibit characteristically large effective masses, magnetic susceptibility χ, and Sommerfeld coefficients of specific heat ($\gamma \geqslant 400$ mJ/mol K^2). Ce_nMIn_{3n+2} (M = Co, Rh, Ir; $n = 1, 2$) is a special family of heavy-fermions that exhibits both magnetism and superconductivity. $CeCoIn_5$ and $CeIrIn_5$ are superconducting at 2.3 and 0.4 K, respectively, while $CeRhIn_5$ superconducts at 2.1 K under applied pressures of 16 kbar [1,2]. At ambient pressure, $CeRhIn_5$ is a heavy-fermion antiferromagnet with an incommensurate magnetic structure and $T_N = 3.8$ K [3]. The electronic specific heat coefficient is $400 \leqslant \gamma \leqslant 700$ mJ/mol K^2.

The $n = 1$ members of the Ce_nMIn_{3n+2} (M = Co, Rh, Ir; $n = 1, 2$) family are layered compounds. The $CeIn_3$ cuboctahedra layers stack periodically with alternating rectangular polyhedra MIn_2 layers along the c-axis [4,5]. A similar arrangement is found in the $n = 2$ subfamily; however, two $CeIn_3$ layers are found for every one MIn_2 layer [6].

The $n = 2$ members of the Ce_nMIn_{3n+2} (M = Co, Rh, Ir; $n = 1, 2$) family have comparable γ values, but Ce_2RhIn_8 orders antiferromagnetically at $T_N = 2.8$ K at ambient pressure. Superconductivity with $T_c \sim 2$ K can be induced with the application of ~ 25 kbar of pressure [7]. Ce_2IrIn_8, on the other hand, remains paramagnetic down to the low temperature.

In our study of ternary intermetallic compounds related to Ce_nMIn_{3n+2} (M = Rh, Ir; $n = 1, 2$), we have found two new compounds $LnPdGa_6$ (Ln = La, Ce). Magnetic and specific heat measurements show an antiferromagnetic heavy-fermion ground state of $CePdGa_6$ due to the f-moments in contrast with its non-magnetic analog, $LaPdGa_6$.

*Corresponding author. Fax: +225-578-3458.
E-mail address: jchan@lsu.edu (J.Y. Chan).

0022-4596/03/$ - see front matter © 2003 Elsevier Inc. All rights reserved.
doi:10.1016/S0022-4596(03)00223-8

2. Experimental

2.1. Synthesis

Single crystals of $CePdGa_6$ and $LaPdGa_6$[1] were grown by the metallic flux method. Ce ingot (3 N, Ames Laboratory), Pd (5 N, Alfa Aesar), and Ga (5 N, Alfa Aesar) or La ingot (3 N, Ames Laboratory), Pd (4 N, Alfa Aesar), and Ga (6 N, Alfa Aesar) were placed into an alumina crucible in a 1:1:20 ratio. The crucible and its contents were then sealed into an evacuated quartz tube and heated to 1150°C. After slowly cooling to 350°C, the tube was inverted and centrifuged to remove the excess flux, and large single crystals of $CePdGa_6$ were left in the crucible. A similar temperature profile was followed for $LaPdGa_6$. Typical crystal size ranged between $5 \times 5 \times 5$ to $10 \times 10 \times 10\ mm^3$. No noticeable degradation of the crystals in air was observed.

2.2. Single-crystal X-ray diffraction

A suitable $0.03 \times 0.05 \times 0.01\ mm^3$ silver-colored fragment was mounted onto the goniometer of a Nonius KappaCCD diffractometer equipped with Mo$K\alpha$ radiation ($\lambda = 0.71073$ Å). High-resolution data were collected up to $\theta = 40.3°$ at 293 K. Further crystallographic parameters are provided in Table 1. The structural model was refined using SHELXL97 [8]. Data were then corrected for extinction and refined with anisotropic displacement parameters. Atomic positions and thermal parameters are provided in Table 2, and selected interatomic distances and bond angles are given in Table 3.

Similar procedures and instrumentation were followed to determine the crystal structure of $LaPdGa_6$. The structure of $CePdGa_6$ served as an initial model for the determination of the crystal structure of the isostructural analog, $LaPdGa_6$.

2.3. Physical property measurements

Magnetization data were obtained using a Quantum Design Magnetic Property Measurement System SQUID magnetometer. The temperature-dependent magnetization data were obtained first under zero-field cooled (ZFC) conditions from 2 to 330 K under a field of 1000 G. Magnetization was then measured while cooling back to 2 K to obtain field-cooled (FC) data. Field (H)-dependent measurements were collected at 2 K with H swept between 0 and 5.5 T. These procedures were followed for fields aligned parallel to the crystallographic a–b plane and c-axis of the crystal.

[1] Supporting information available: Crystallographic data in CIF format are available for $CePdGa_6$ and $LaPdGa_6$.

Table 1
Crystallographic parameters

	Formula	
	$CePdGa_6$	$LaPdGa_6$
Crystal data		
a(Å)	4.350(3)	4.3760(3)
c(Å)	7.922(6)	7.9230(5)
V(Å^3)	149.90(19)	151.721(18)
Z	1	1
Crystal dimension (mm^3)	$0.03 \times 0.05 \times 0.10$	$0.01 \times 0.08 \times 0.08$
Crystal system	Tetragonal	Tetragonal
Space group	$P4/mmm$	$P4/mmm$
θ range (°)	2.5–40.4	2.5–33.14
μ (mm^{-1})	36.73	35.829
Data collection		
Measured reflections	937	537
Independent reflections	327	215
Reflections with $I > 2\sigma(I)$	317	205
R_{int}	0.082	0.1456
h	$-7 \rightarrow 7$	$-6 \rightarrow 6$
k	$-5 \rightarrow 5$	$-4 \rightarrow 4$
l	$-12 \rightarrow 14$	$-12 \rightarrow 10$
Refinement		
$R[F^2 > 2\sigma(F^2)]$[a]	0.036	0.0538
w$R(F^2)$[b]	0.089	0.1421
Reflections	327	215
Parameters	13	13
$\Delta\rho_{max}$ (e Å^{-3})	3.65	4.18
$\Delta\rho_{min}$ (e Å^{-3})	−1.96	−4.06
Extinction coefficient	0.021(3)	0.027(8)

[a] $R_1 = \sum ||F_o| - |F_c|| / \sum |F_o|$
[b] w$R_2 = \sum [w(F_o^2 - F_c^2)] / \sum [w(F_o^2)^2]^{1/2}$

Specific heat was measured by a thermal relaxation method down to 0.35 K.

3. Results and discussion

3.1. Structure

LnPdGa$_6$ (Ln = La, Ce) crystallize in the tetragonal $P4/mmm$ space group (No. 123) with the Ln, Pd, Ga1, and Ga2 occupying the 1a, 1b, 2h, 4i sites, respectively.

The crystal structure of $CePdGa_6$ bears a striking resemblance to the heavy-fermion family of compounds, CeMIn$_5$ (M = Co, Rh, Ir). CeMIn$_5$ and LnPdGa$_6$ (Ln = La, Ce) share the same $P4/mmm$ space group and similar lattice parameters ($\sim 4 \times 7$ Å). The structure of CeMIn$_5$ can be viewed as a periodic stacking of CeIn$_3$ cuboctahedra layers and MIn$_2$ layers along the c-axis. In $CePdGa_6$, however, the coordination of the Ce atom results in face-sharing 8-coordinate $CeGa_{8/4}$ rectangular prisms instead of 12-coordinate cuboctahedra. In addition, the $CeGa_{8/4}$ rectangular prisms are staggered with the edge-sharing $PdGa_{8/2}$

Table 2
Atomic positions and thermal parameters of LnPdGa$_6$ (Ln = La, Ce)

Atom		x	y	z	U_{11}	U_{22}	U_{33}
CePdGa$_6$							
Ce	1*a*	0	0	0	0.0117(2)	0.0117(2)	0.0161(3)
Pd	1*b*	0	0	1/2	0 .0122(3)	0.0122(3)	0.0153(4)
Ga1	2*h*	0.5	0.5	0.15149(13)	0.0154(3)	0.0154(3)	0.0121(4)
Ga2	4*i*	0	0.5	0.32935(9)	0.0138(3)	0.0166(3)	0.0124(3)
LaPdGa$_6$							
La	1*a*	0	0	0	0.0134(5)	U_{11}	0.0099(7)
Pd	1*b*	0	0	1/2	0.0138(6)	U_{11}	0.0109(8)
Ga1	2*h*	1/2	1/2	0.15263(17)	0.0174(7)	U_{11}	0.074(8)
Ga2	4*i*	1/2	0	0.33040(12)	0.0147(7)	0.0180(7)	0.0070(7)

Table 3
Select interatomic distances and bond angles of LnPdGa$_6$ (Ln = La, Ce)

	CePdGa$_6$	LaPdGa$_6$
Within LnGa$_4$ rectangular prisms		
Ln–Ga1 (×8)(Å)	3.3017(4)	3.3222(5)
Ga1–Ga1 (×4)(*c*-axis)(Å)	2.400(2)	2.419(3)
Ga1–Ga1 (×4)(*a*–*b* plane)(Å)	4.350(6)	4.351(8)
	Angles (°)	
Ga1–Ce–Ga1	42.63(3)	42.69(4)
	82.408(12)	82.386(15)
Within PdGa$_2$ rectangular prisms		
Pd–Ga2 (×8)(Å)	2.5609(4)	2.5677(5)
Ga1–Ga1 (×4)(*c*-axis)(Å)	2.7039(15)	2.6875(19)
Ga1–Ga1 (×4)(*a*–*b* plane)(Å)	3.076(6)	3.076(7)
	Angles (°)	
Ga2–Pd–Ga2	63.742	63.11(4)
	73.812	74.105(17)

rectangular prism layer by 90°. The structures of $CeCoIn_5$ and $CePdGa_6$ are provided in Fig. 1.

The Pd–Ga interatomic distance found in the $PdGa_2$ prisms is 2.5609(4) Å, which agrees with other known Pd–Ga distances. In Pd_2Ga, for example, Pd and Ga atoms are separated by 2.558 Å. The Pd–Ga distances in Pd_5Ga_3 range between 2.388–2.701 Å [9], and 2.501–2.691 Å in $PdGa_5$ and Pd_2Ga [10]. In addition, the sum of the two covalent radii of Ga (1.22 Å) and Pd (1.37 Å) gives an expected interatomic distance of 2.59 Å, which is close to our experimental Pd–Ga distance of 2.5609(4) Å [11].

The Ce–Ga distance in the $CeGa_4$ prisms in $CePdGa_6$ is 3.3017(4) Å, which is slightly larger than the 3.252–3.299 Å range of Ce–Ga distances found in $CeGa_2$ [12], Ce_5Ga_3, and $CeGa_6$ [12]. However, all of these values are slightly larger than 3.04 Å, the bond length estimated by summing the Ce (1.82 Å) and Ga (1.22 Å) covalent radii [11].

In the layer of $CeGa_4$ prisms in $CePdGa_6$, the Ga–Ga distance along the *a*–*b* plane is 4.350(6) Å. The Ga–Ga distance measures 2.400(2) Å along the *c*-axis, which is close to 2.442 Å, the bond distance based on the Ga covalent radius (1.22 Å). The length along the *c*-axis of the $PdGa_2$ layer is 2.7039(15) Å. Both Ga–Ga distances fall within a range of 2.297–2.930 Å found in $CeGa_6$ [12], $CeGa_2$ [12], and $PdGa_5$ [10].

The Ga–Ga distance between the $LnGa_{8/4}$ and $PdGa_{8/2}$ layers is ~2.56 Å. This is slightly longer than the expected 2.4 Å Ga–Ga bond distance based on the covalent radii mentioned previously. In addition, the Ce–Ga2 interatomic distance measures 3.3967(6) Å, which is slightly longer than the Ce–Ga1 distances of the typical Ce–Ga bond distance range of 3.252–3.299 Å. Theoretical calculations will be performed in order to provide further insights into the true bonding of this material.

Similar yet slightly larger Ce–Ga and Ga–Ga interatomic distances are found in the isostructural $LaPdGa_6$ analog, which is expected due to lanthanide contraction. Further crystallographic parameters for the La analog are provided in Tables 2 and 3.

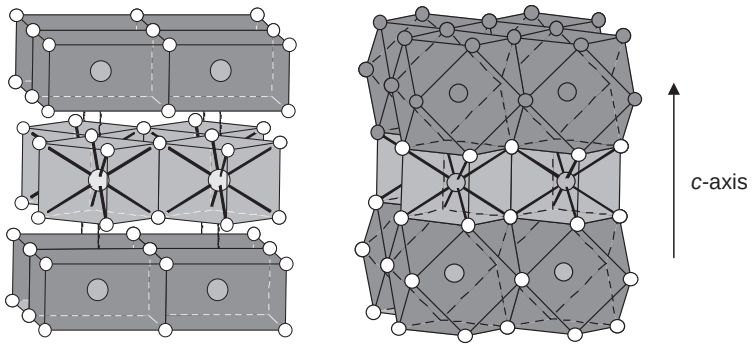

Fig. 1. The crystal structure of (a) $CePdGa_6$ and (b) $CeCoIn_5$ are shown along the c-axis. (a) The face-sharing Ce rectangular prisms are shaded dark gray; the edge-sharing Pd rectangular prisms are shaded light gray, and Ga atoms are shown as white circles. (b) Ce cuboctahedra, shaded in dark gray, alternate along the c-axis with Pd rectangular prisms, shaded in light gray. In atoms are shown as white circles.

3.2. Physical properties

Fig. 2 shows the temperature dependence of the specific heat C/T for $CePdGa_6$ and $LaPdGa_6$. A sudden jump at $T_N = 10$ K and a small anomaly at 5 K are observed in the specific heat, indicating a double transition. The f-electron contribution to the specific heat, C_m/T, is obtained by subtracting C/T of $LaPdGa_6$, as shown in the inset of Fig. 2. For $T > T_N$, the electronic specific heat coefficient γ of $CePdGa_6$ varies very little between ~ 230 and 300 $mJ/mol\,K^2$. Furthermore, γ remains large at ~ 160 $mJ/mol\,K^2$, even at 0.4 K when $CePdGa_6$ is in the ordered state.

Fig. 3 presents the temperature-dependence of the susceptibility of $CePdGa_6$ along the a–b plane and along the c-axis. Data for both orientations follow Curie–Weiss behavior above 10 K with effective moments of 2.53 μ_B (a–b plane) and 2.32 μ_B (c-axis), and Weiss temperatures (Θ_W) of 1.84 K (a–b plane) and 18.06 K (c-axis). As expected from the positive values for Θ_W, the overlap between the field-cooled and zero-field cooled measurements along the a–b plane show similar behavior. At 10 K, there is a cusp in the c-axis component of the magnetic susceptibility, followed by a decrease in the susceptibility at low temperatures. This feature is typical of antiferromagnetic transitions. When the field is applied along the a–b plane, however, different magnetic behavior is observed; both results for the field-cooled and zero-field cooled measurements along the a–b plane show similar behavior. This suggests that the anomalous peak at 5 K is indicative of ferromagnetic ordering and agrees with the lower ordering temperature determined from the specific heat. The strong anisotropy should be noted; no anomaly was found in the measurements along the c-axis component at this temperature. This is probably due to a reconfiguration of the magnetic structure. Most likely, antiferromagnetic ordering occurs at 10 K with the spins along the c-axis, but the canting of the spins at 5 K generates a net ferromagnetic moment along the a–b plane. Neutron diffraction measurements will be performed to elucidate the precise magnetic structure. We have also measured the susceptibility of $LaPdGa_6$ (not shown), and found non-magnetic behavior ($\chi = -10^{-4}$ emu/mol at 273 K). This suggests that the magnetic moments result only from the Ce f-electron, not from Pd d-electrons.

Field-dependent magnetization measurements were made to further characterize $CePdGa_6$. The magnetization of a single crystal of $CePdGa_6$ with the c-axis and a–b plane oriented parallel to the field is shown as a function of field in Fig. 4. With the field parallel to the c-axis, the magnetization increases steadily with field. At 2 T, there is a rapid increase in magnetization until ~ 3 T where the change in slope indicates a saturation in magnetization. The rapid increase in magnetization at 2 T is a clear indication of a metamagnetic transition occurring along the c-axis, most likely due to a spin–flip transition. No metamagnetic transition was observed with the field oriented along the crystallographic a–b plane and only a small spontaneous moment of ~ 0.05 μ_B was found. The fact that this moment is two orders of magnitude smaller than that expected for Ce^{3+} also support the canting of the spins. Hysteresis is observed in the metamagnetic transition region for the field applied along the c-axis and at low fields (0.7 T) along the a–b plane.

The strong magnetic anisotropy, observed in the T and H dependence of the magnetization, should originate from its unique layered structure. If one considers the differences in the Ce–Ce distances (4.350(3) Å along the a–b plane and 7.922(6) Å along the c-axis), the magnetic correlations in the a–b plane should be stronger than those along the c-axis. In addition, the sign of the coupling may be different; the Ce moments along the a–b plane correlate

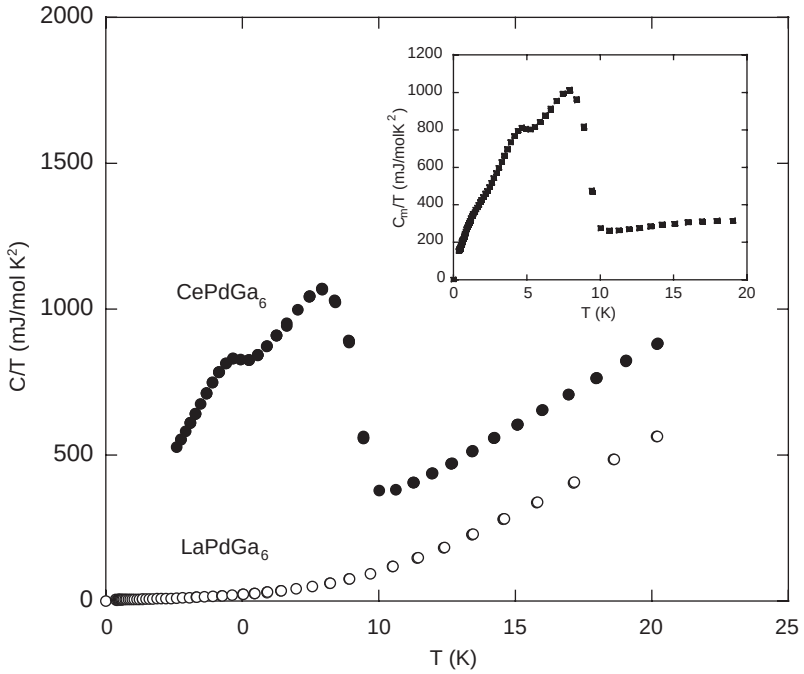

Fig. 2. The zero-field specific heat C/T vs. T are shown for both $CePdGa_6$ (solid circle) and $LaPdGa_6$ (open circle). The inset shows the T dependence of the f-electron contribution C_m/T for $CePdGa_6$.

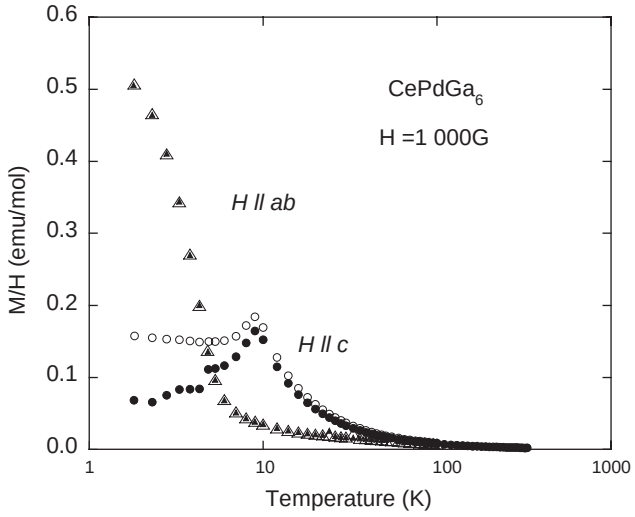

Fig. 3. Magnetic susceptibility M/H as a function of T where open circles are for applied field parallel to the crystallographic c-axis and triangles are for applied field parallel to the crystallographic a–b plane. Closed symbols are for ZFC measurements and open symbols are for FC measurements.

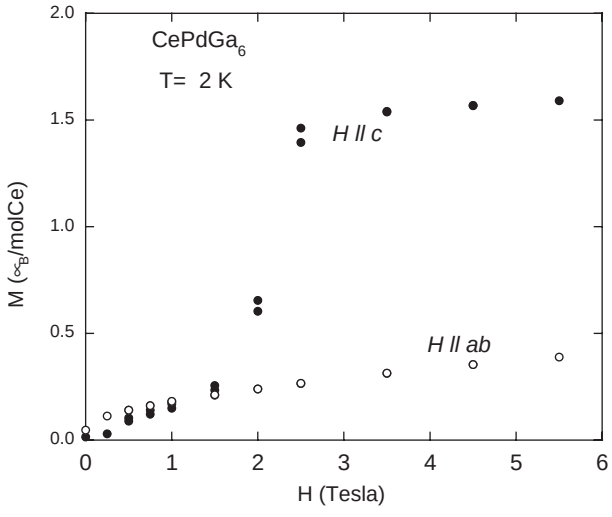

Fig. 4. Magnetization as a function of H, measured at 2 K. Closed and open circles represent data collected for fields applied parallel to the crystallographic c-axis and a–b plane, respectively.

antiferromagnetically, while the Ce moments along the c-axis correlate ferromagnetically. The difference in both sign and magnitude of the coupling may be the origin of the complex and strong anisotropy found in the magnetic data. Furthermore, the appearance of magnetism in a heavy-electron state, similar to Ce_nMIn_{3n+2} $(M = Co, Rh, Ir; n = 1, 2)$, indicates competition between RKKY interactions and Kondo coupling. The relatively large $\gamma \sim 160\ mJ/mol\ K^2$, even at 0.4 K, suggests a strong Kondo effect in the ordered state. Therefore, the metamagnetism observed at 2 K may originate not only from a spin–flip transition, but also from the simultaneous collapse of the Kondo screening effect in the field. These interesting features suggest a rich field of magnetism in this new structural class of materials.

Considering their structural and obvious chemical similarity to the $LnMX_5$ compounds, unusual physical properties, such as superconductivity, may exist in this new family of $LnMX_6$ materials. Further exploration of the magnetic and transport properties, such as chemical pressure/doping effects to the magnetic heavy-fermion state, of LnPdGa$_6$ series is currently in progress. In addition, the effects of substitutions of other lanthanide elements will be investigated.

Acknowledgments

J.Y.C. acknowledges Louisiana Board of Regents, PRF-G, and NSF DMR-0237664 and Z.F. acknowledges NSF DMR-9971348 for partial support of this project.

References

[1] C. Petrovic, P.G. Pagliuso, M.F. Hundley, R. Movshovich, J.L. Sarrao, J.D. Thompson, Z. Fisk, P. Monthoux, J. Phys.: Condens. Matter 13 (2001) L337.
[2] C. Petrovic, R. Movshovich, M. Jaime, P.G. Pagliuso, M.F. Hundley, J.L. Sarrao, Z. Fisk, J.D. Thompson, Europhys. Lett. 53 (2001) 354.
[3] H. Hegger, E.G. Moshopoulou, M.F. Hundley, J.L. Sarrao, Z. Fisk, J.D. Thompson, Phys. Rev. Lett. 84 (2000) 4986.
[4] E.G. Moshopoulou, Z. Fisk, J.L. Sarrao, J.D. Thompson, J. Solid State Chem. 158 (2001) 25.
[5] E.G. Moshopoulou, J.L. Sarrao, P.G. Pagliuso, N.O. Moreno, J.D. Thompson, Z. Fisk, R.M. Ibberson, Appl. Phys. A Mater. Sci. Proc. 74 (2001) s895.
[6] R.T. Macaluso, J.L. Sarrao, N.O. Moreno, P.G. Pagliuso, J.D. Thompson, F.R. Fronczek, M.F. Hundley, R. Movshovich, J.Y. Chan, Chem. Mater. 15 (2003) 1394.
[7] M. Nicklas, V.A. Sidorov, H.A. Borges, P.G. Pagliuso, C. Petrovic, Z. Fisk, J.L. Sarrao, J.D. Thompson, arXiv: cond-mat/0204064.
[8] G.M. Sheldrick, SHELXL97, University of Göttingen, Germany, 1997.
[9] S. Bhan, H. Kudielka, Z. Metallkd. 69 (1978) 333.
[10] K. Schubert, H.L. Lukas, H.-G. Meissner, S. Bhan, Z. Metallkd. 50 (1959) 534.
[11] L. Sutton, Tables of Interatomic Distances and Configurations in Molecules and Ions, Vol. Spec. Publ. No. 18, The Chemical Society, London, 1965.
[12] G. Kimmel, D. Dayan, A. Grill, J. Pelleg, J. Less-Common Metals 75 (1980) 133.